Large Synoptic Survey Telescope

Supernovae and Cosmic Shear as Complementary Probes of Dark Energy

L. Knox (UC Davis), A. Albrecht (UC Davis), Y.-S. Song (U Chicago), J.A. Tyson (UC Davis), D. Wittman (UC Davis)

Abstract

Weak lensing observations and supernova observations, combined with CMB observations, can both provide powerful constraints on dark energy properties. We find luminosity distances inferred from 2000 supernovae and large-scale (l < 1000) angular power spectra inferred from redshift-binned cosmic shear maps of half of the sky place complementary constraints on w_0 and w_a where $w(z) = w_0 + w_a(1-a)$. Further, each set of observations constrains higher-dimensional parameterizations of w(z) and constrains these in different ways. To quantify these abilities we consider eigenmodes of the w(z) error covariance matrix. The best-determined mode for each dataset has a standard deviation of about 0.03. This error rises quite slowly with increasing eigenmode number for the lensing data, reaching one only by the 7th mode. The eigenmode shape differences indicate that lensing is better at probing higher z while supernovae have their chief advantage at lower z.

1. Introduction

- **Complementary Probes** Given the importance of the dark energy mystery and the challenges to constraining its properties, the diversity of methods to probe it is a blessing. Here we concentrate on two methods: weak lensing shear power spectra vs redshift and supernova luminosity distances vs redshift. Each of these very different types of observations are potentially powerful probes of dark energy. In particular we examine the complementary nature of their statistical errors. See the following two posters for complementary weak lens methods.

2. Models of the Data

- **Cosmic Shear** For the 20,000 deg^2 LSST weak lens survey, we assume a galaxy redshift distribution for a limiting magnitude in R of 26 inferred from observations with the Subaru telescope (Nagashima et al. 2002). The shape of this distribution is well-described by the following analytic form:

  $dn/dz \,/\, z^{1.3}\exp[-(z/1.2)^{1.2}]$ for $z < 1$

  $dn/dz \,/\, z^{1.1}\exp[-(z/1.2)^{1.2}]$ for $z > 1$.

  We use this distribution with the modification that half of the galaxies in the $1.2 < z < 2.5$ range are discarded as undetectable. The amplitude of the distribution is such that, after this cut, the number density of galaxies is 65 per sq. arcmin.

  We further assume that the galaxies can be divided, by photometric redshift estimation, into eight different redshift bins: [0-0.4], ..., [2.8-3.2] and that for angular frequencies $40 < l < 1000$ systematic errors are small. While this last assumption is consistent with recent data from new technology telescopes (see Claver etal poster), all-sky simulations will be necessary. Finally, we assume that the shape noise (expressed as a per-component rms shear) is given by $\gamma_{rms}(z) = 0.15+0.035z$.

  For more on data modeling, see Song & Knox (2003).

- **Supernovae.** For the supernova survey we assume 2000 distributed in redshift as described in Kim et al. 2004 as a baseline SNAP supernova survey. In addition, we assume measurement of 100 local supernovae. To our cosmological parameter set, detailed below, we add a supernova luminosity calibration parameter.

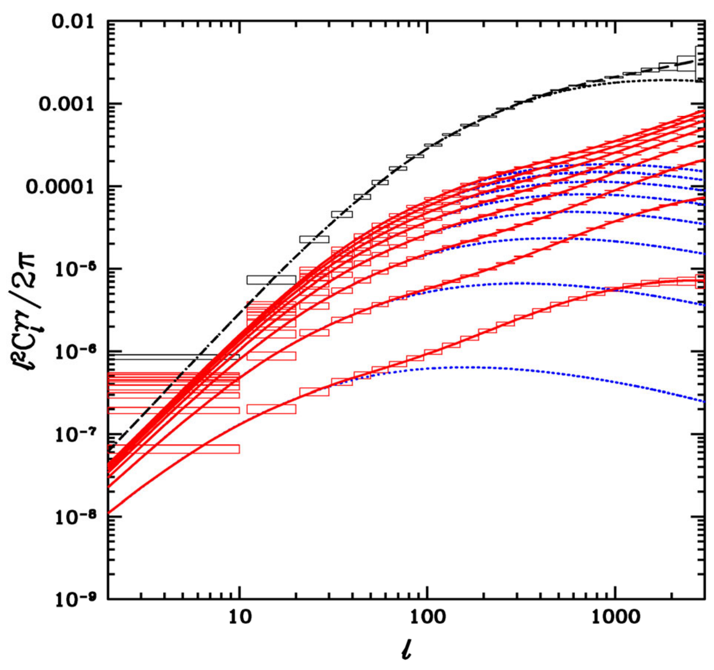

Figure 1: Shear Power Spectra *The shear-shear auto power spectra. The 8 solid curves are the shear power spectra from each of the eight galaxy source planes. Dotted curves are the linear perturbation theory approximation. The source plane redshift intervals are all of width 0.4 and are centered on, from bottom top: 0.2, 0.6. 1.0, 1.4, 1.8, 2.2, 2.6 and 3.0. The error boxes are forecasts for LSST. The top dashed curve is the shear power spectrum for the CMB source plane. The error boxes are forecasts for CMBpol.*

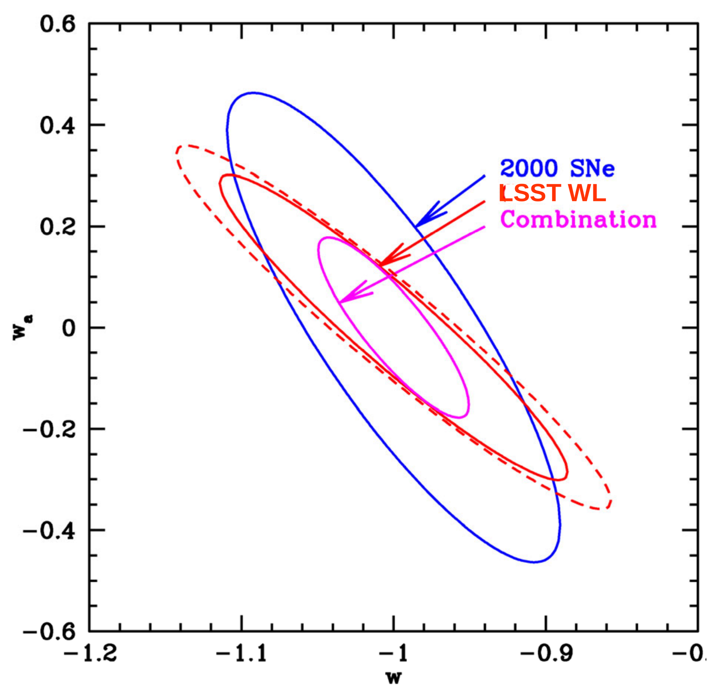

Figure 2: w_0 & w_a Error Forecasts *One sigma error contours in the w_0-w_a plane for LSST shear survey, 2000 SNe, and the combination (as labeled) where $w(z) = w_0+w_a(1-a)$. The dashed curve is for LSST with the source density uniformly decreased by a factor of 2. These same shear data can be analyzed with other statistics such as three-point correlations (Jarvis and Takada posters),and mass cluster counts (Haiman poster), collectively yielding higher precision.*

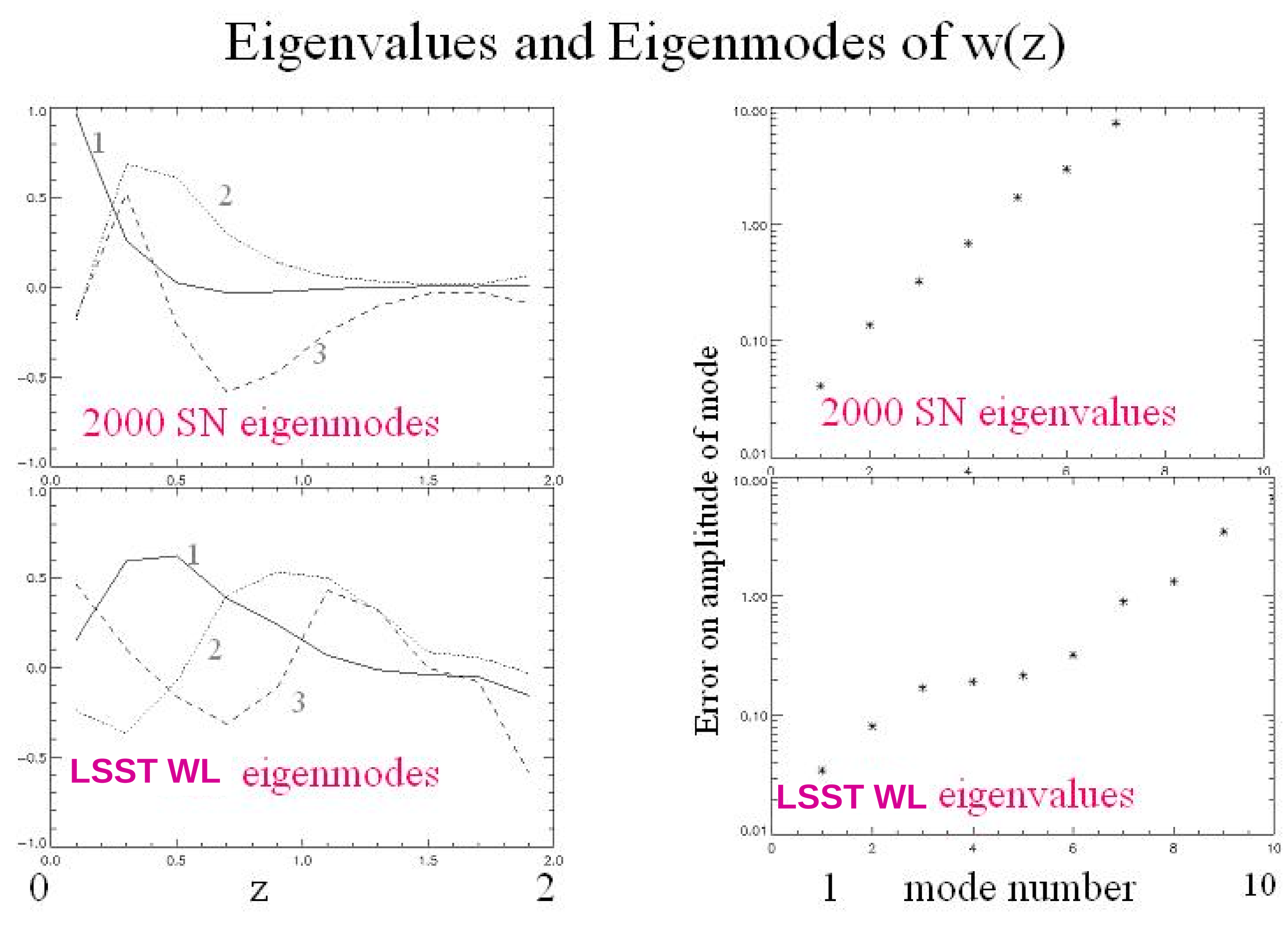

Figure 3. *Eigenvalues and first three eigenmodes of the w(z) error covariance matrix for LSST WL+Planck and 2000 SNe+Planck. The large contributions to the eigenmodes from the highest redshift-bin are an artifact of that bin being much broader than the rest, extending all the way to the last-scattering surface.*

3. Models of Cosmology

- **The Parameter Set.** We take our (non-w(z)) set to be P = $\{w_m, w_b, w_n, q_s, z_{ri}, k^3P_F^i(k_f), n_s, n_s', y_{He}\}$, with the assumption of a flat universe. The first three of these are the densities today (in units of 1.88×10^{-29}g/cm^3) of cold dark matter + baryons, baryons, and massive neutrinos. We assume two massless species and one massive species. The next is the angular size subtended by the sound horizon on the last-scattering surface. The Thompson scattering optical depth for CMB photons, t, is parameterized by the redshift of reionization z_{ri}. The primordial potential power spectrum is assumed to be a near power-law with spectral index $n_s(k) = n_S(k_f) + n_S'\ln(k/k_f)$ and $k_f = 0.05$ Mpc^{-1}. The fraction of baryonic mass in Helium (which affects the number density of electrons) is y_{He}. We Taylor expand about P = {0.146, 0.021, 0, 0.6, 6.3, 6.4 x 10^{11}, 1, 0, 0.24}. The Hubble constant for this model is H_0 = 65.5 km/s/Mpc.
- **w(z) in redshift bins.** To deepen our understanding of how these surveys are constraining dark energy, we have examined how they constrain the function w(z), rather than its simple parameterization by w_0 and w_a. We proceed by binning w(z) in redshift bins and then identifying the eigenmodes and eigenvalues of the binned w(z) error covariance matrix as was done for supernovae by Huterer & Starkman (2003).

4. Results

We particularly emphasize the eigenmode/eigenvalue results from our analysis of the statistical errors. We see a striking difference in the modes for 2000 SNe vs. the modes for LSST WL: those for LSST stretch out to higher z. The reason for this is that lensing is less sensitive to the growth factor at the lower redshifts where the source density in a given redshift bin is small and the lensing window (for sources at higher z) is also small. Thus the supernovae are better at detecting changes in w(z) at lower z and LSST shear tends to be better at detecting changes at higher redshift.

LSST and 2000 SNe also have strikingly different eigenvalue spectra. The error on the amplitude of the best determined mode is quite similar for each ~0.03. But the 2000 SNe spectrum is much steeper. LSST has six modes with sigma < 0.5, whereas 2000 SNe has three.